

Controlling the Transmission Dynamics of Lassa Fever through Integrated Control Strategies

Silas Daniel and Zainab Ali Mohammed

Department of Mathematics, Adamawa State University, Mubi, Nigeria

Date of Submission: 23-01-2026

Date of Acceptance: 05-02-2026

Abstract

Lassa fever continues to pose a major public health threat in West Africa, particularly in Nigeria where the disease remains endemic. This study presents a comprehensive two-host mathematical model that captures the transmission dynamics of Lassa fever among humans, rodents, and the environment. The model incorporates asymptomatic human infection and dual environmental contamination pathways (through contaminated items and aerosols). Four intervention strategies are integrated: surveillance and case detection, infection control, public health education, and rodent-targeted control. Analytical results establish the positivity and boundedness of solutions, derive the disease-free equilibrium (DFE), compute the basic and controlled reproduction numbers, and determine local and global stability conditions using the next-generation matrix and Routh–Hurwitz criteria. Numerical simulations reveal that combined interventions substantially reduce the infection burden in both humans and rodents, as well as environmental viral load. The controlled reproduction number decreases from $R_0 \approx 2.47$ (baseline) to $R_c \approx 0.52$ under high control intensity, indicating potential disease elimination. The results emphasize that sustained surveillance, effective isolation, public awareness, environmental sanitation, and rodent population management are critical for long-term control and eventual eradication of Lassa fever in endemic regions.

Keywords: Lassa fever; asymptomatic infection; environmental contamination; mathematical modeling; control strategies; stability analysis; simulation.

1. Introduction

Lassa fever is a severe viral hemorrhagic illness endemic to West Africa, with Nigeria reporting the majority of annual cases and fatalities. The disease is caused by the Lassa virus, a member of the *Arenaviridae* family, and is primarily transmitted to humans through contact with food or household items contaminated with the urine or feces of infected *Mastomys natalensis* rodents, the natural reservoir of the virus. Secondary human-to-human transmission also occurs, particularly among healthcare workers and family members caring for infected patients. Despite decades of research and recurrent outbreaks, Lassa fever remains a major public health challenge due to persistent rodent–human contact, poor environmental hygiene, and inadequate healthcare infrastructure in rural and peri-urban communities of Nigeria (WHO, 2023, NCDC, 2024).

The Lassa virus exhibits complex transmission dynamics involving three primary routes: zoonotic transmission from infected rodents, direct human-to-human transmission, and indirect environmental transmission through contaminated surfaces or aerosolized particles. Environmental persistence of the virus plays an important role in sustaining outbreaks even when rodent populations are temporarily reduced. Recent reports by the Nigeria Centre for Disease Control (NCDC) highlight the increasing number of cases linked to healthcare-associated infections, emphasizing the need for comprehensive and integrated control strategies that combine medical, behavioral, and environmental interventions.

Mathematical modeling provides a powerful approach to understanding infectious disease

dynamics, predicting epidemic trends, and designing effective control measures. Models serve as simplified representations of real-world disease processes, allowing the assessment of intervention outcomes under various epidemiological and demographic conditions. In the case of Lassa fever, modeling efforts have helped explain the interplay between human and rodent populations, environmental contamination, and the effectiveness of control strategies such as sanitation, public awareness, and case isolation (Iboi et al. , 2020, Adegboye et al., 2022).

Traditional Lassa fever models have often focused on the direct transmission between rodents and humans, neglecting the indirect role of environmental reservoirs and the impact of asymptomatic infections. Asymptomatic individuals, although less infectious than symptomatic cases, can still contribute significantly to disease persistence by sustaining low-level transmission that is difficult to detect through conventional surveillance. Moreover, previous models rarely combined multiple realistic control measures within a unified framework, limiting their applicability for long-term policy evaluation.

To address these gaps, this study develops a deterministic two-host Lassa fever model that explicitly incorporates asymptomatic human infection, dual environmental contamination pathways (through items and aerosols), and four control strategies: surveillance and case detection, infection control, public health education, and rodent-targeted intervention. The model aims to provide a comprehensive understanding of the joint effects of these controls on disease transmission, persistence, and eradication thresholds.

The results from this study are expected to offer theoretical insight into the combined impact of human behavior, environmental hygiene, and rodent management on Lassa fever dynamics. By evaluating the reproduction number and stability properties, and through numerical simulations, the study demonstrates how coordinated control measures can effectively suppress outbreaks and

promote long-term elimination of the disease in endemic settings such as Nigeria.

2. Literature Review

Lassa fever has attracted significant epidemiological and modeling attention since its identification in the 1960s, primarily due to its recurrent outbreaks and high mortality rate in endemic regions of West Africa. Numerous studies have investigated its virology, clinical presentation, transmission mechanisms, and control strategies. Recent developments in mathematical modeling have further improved our understanding of how human, rodent, and environmental factors interact to sustain disease transmission.

Early epidemiological investigations established that the multimammate rat (*Mastomys natalensis*) acts as the principal reservoir of the Lassa virus (Gibb et al., 2017). Humans are typically infected through the ingestion or inhalation of materials contaminated with rodent excreta, and secondary infections occur through human-to-human contact, particularly in healthcare settings where infection prevention measures are weak. Given the persistence of Lassa virus in rodent populations and contaminated environments, elimination efforts must combine both public health and ecological control strategies.

Several deterministic models have been proposed to study the dynamics of Lassa fever transmission. Gibb et al. (2017) explored rodent ecology and demonstrated how fluctuations in population density influence spillover risks to humans. Iboi et al. (2020) developed a human-rodent model that included time-dependent control variables such as education and sanitation, showing that early implementation of control strategies substantially reduces infection prevalence. Adegboye et al. (2022) extended this approach by incorporating environmental contamination, highlighting the role of indirect transmission pathways in sustaining outbreaks.

Despite these advances, several research gaps remain. Most existing models treat all infected humans as a single homogeneous class, overlooking the epidemiological importance of asymptomatic

infections. In reality, many Lassa fever cases are mild or subclinical and may not be detected through routine surveillance, yet such cases can still contribute to viral shedding and transmission. The failure to account for these hidden carriers can lead to underestimation of the basic reproduction number and misjudgment of control requirements.

Environmental factors are another critical component often simplified in previous studies. While some models consider a single environmental compartment, empirical evidence suggests that Lassa virus survival differs between contaminated surfaces and airborne particles. The distinction between these two reservoirs (contaminated items and contaminated aerosols), provides a more realistic framework to assess indirect transmission and environmental control effectiveness.

In terms of control strategies, earlier mathematical studies commonly focused on single or dual interventions such as isolation or sanitation. However, effective control of Lassa fever requires a multifaceted approach that integrates active case detection, community education, infection control within health facilities, and rodent-targeted environmental management. Few models have captured the joint effect of these interventions, particularly when they interact through overlapping transmission routes.

The current study builds upon these foundations by constructing a comprehensive twohost, multi-pathway model that includes asymptomatic infection and explicitly models environmental contamination through both fomites and aerosols. In addition, it introduces four control strategies: surveillance and case detection,

infection control, public health education, and rodent-targeted interventions. This integration enables a holistic assessment of how human behavior, medical intervention, and ecological management jointly influence the reproduction number (R_0), disease persistence, and the likelihood of eradication.

3.0 Materials and Methods

3.1 Model Formulation

We consider a Lassa fever model consisting of two interacting host populations: humans and rodents. The human population is divided into susceptible (S_h), exposed (E_h), symptomatic infectious (I_h), and asymptomatic infectious (A_h), quarantined (Q_h), and recovered (R_h) compartments. The rodent population is divided into susceptible (S_r) and infectious (I_r) classes. We have included environmental contamination as transmission pathway, thereby adding environment-human and rodents' pathways. The environmental contamination is divided into: contaminated items (C_I) and contaminated air or aerosols (C_A). Symptomatic humans (I_h), asymptomatic humans (A_h), and infectious rodents

(I_r) shed Lassa virus into both surface or items and air reservoirs at rates $\sigma_{Ih}, \sigma_{Ah}, \sigma_{Ir}$ (surface shedding) and $\zeta_{Ih}, \zeta_{Ah}, \zeta_{Ir}$ (aerosol shedding). Decay, cleaning, and ventilation remove contamination at rates ω_I and ω_A , respectively.

3.2 Model variables and parameters

The variables as well as the parameters used for our model, together with their descriptions and biological meanings are found in Table 1 and Table 2 respectively.

Table 1: Description of model variables.

Variable	Description	Population
S_h	Susceptible humans	Human
E_h	Exposed (latent) humans	Human
I_h	Symptomatic infectious humans	Human
A_h	Asymptomatic infectious humans	Human
Q_h	Quarantined or isolated humans	Human
R_h	Recovered (immune) humans	Human
S_r	Susceptible rodents	Rodent
I_r	Infectious rodents	Rodent
C_I	Contaminated items (fomites, surfaces, food)	Environment
C_A	Contaminated air or aerosols	Environment

Table 2: Description of model parameters and their biological meanings.

Parameter	Description	Typical unit/value
Λ_h	Recruitment rate of humans	persons/day
Λ_r	Recruitment rate of rodents	rodents/day
μ_h	Natural death rate of humans	day ⁻¹
μ_r	Natural death rate of rodents	day ⁻¹
κ_h	Progression rate from exposed to infectious	day ⁻¹
p	Proportion of exposed humans who become asymptomatic	dimensionless
γ_{Ih}	Recovery rate of symptomatic humans	day ⁻¹
γ_{Ah}	Recovery rate of asymptomatic humans	day ⁻¹
δ_h	Disease-induced death rate in humans	day ⁻¹
ϕ_{Ih}	Quarantine rate of symptomatic humans	day ⁻¹
ϕ_{Ah}	Quarantine rate of asymptomatic humans	day ⁻¹
η_{Qh}	Recovery rate of quarantined humans	day ⁻¹
σ_{Ih}	Shedding rate from infectious humans to items	day ⁻¹
σ_{Ah}	Shedding rate from asymptomatic humans to items	day ⁻¹
σ_{Ir}	Shedding rate from infectious rodents to items	day ⁻¹
ζ_{Ih}	Aerosol shedding rate from infectious humans	day ⁻¹
ζ_{Ah}	Aerosol shedding rate from asymptomatic humans	day ⁻¹
ζ_{Ir}	Aerosol shedding rate from infectious rodents	day ⁻¹
ω_{CI}	Decay rate of contamination on items	day ⁻¹
ω_{CA}	Decay rate of contamination in air/aerosols	day ⁻¹
β_{hh}	Transmission rate human-to-human	day ⁻¹
β_{ha}	Transmission rate asymptomatic-to-human	day ⁻¹
β_{rh}	Transmission rate rodent-to-human	day ⁻¹
β_{rr}	Transmission rate rodent-to-rodent	day ⁻¹
β_{CIh}	Transmission rate environment (items) to human	day ⁻¹
β_{CAh}	Transmission rate aerosols to human	day ⁻¹
β_{CIr}	Transmission rate environment (items) to rodent	day ⁻¹
β_{CAr}	Transmission rate aerosols to rodent	day ⁻¹
c_r	Rate of rodent-targeted control removal	day ⁻¹
$u_1(t)$	Surveillance and case detection control	dimensionless
$u_2(t)$	Infection control (hygiene/sanitation)	dimensionless
$u_3(t)$	Public health education control	dimensionless
$u_4(t)$	Rodent-targeted control	dimensionless

3.3 Model assumptions

The model is formulated based on the following biologically reasonable assumptions:

1. The total human and rodent populations are denoted by $N_h(t) = S_h + E_h + I_h + A_h + Q_h + R_h$ and $N_r(t) = S_r + I_r$, respectively.
2. Recruitment into the human and rodent populations occurs at constant rates Λ_h and Λ_r , respectively, and all individuals experience natural deaths at rates μ_h and μ_r .
3. Exposed humans (E_h) are latently infected but not infectious. After an average incubation period $1/\kappa_h$, a fraction $(1 - p)$ progress to the symptomatic class (I_h), while a fraction p progress to the asymptomatic class (A_h).
4. Asymptomatic humans (A_h) are infectious but with reduced transmissibility compared to symptomatic individuals.
5. Infected humans (I_h and A_h) may be detected and isolated through surveillance and case finding at rates ϕ_{I_h} and ϕ_{A_h} , respectively. The detection efficiency is enhanced by the control effort u_1 .
6. Quarantined individuals (Q_h) recover at rate η_{Q_h} , and both quarantined and infectious individuals may experience disease-induced deaths at rates δ_h and δ_{Q_h} .
7. Infected rodents (I_r) remain infectious throughout their lifetime; they do not recover. Rodent-targeted control, denoted by u_4 , increases the removal rate of infected rodents (e.g., through rodent-proofing, environmental sanitation, baiting, or trapping).
8. Both infectious humans and rodents contribute to environmental contamination through shedding into contaminated items (C_I) and contaminated air/aerosols (C_A). Environmental shedding is reduced proportionally by the infection-control effort u_2 .

9. Public health education (u_3) reduces all effective contact rates, thus lowering the forces of infection for both hosts.
10. The environmental compartments do not contribute to new infections directly in the computation of \mathcal{R}_0 , since they act as passive reservoirs of infection.

3.4 Model schematic diagram

The flow or schematic diagram of the model, showing the different interactions, transitions or change of states, as well as the shedding of the virus to the environment is given in Figure 1.

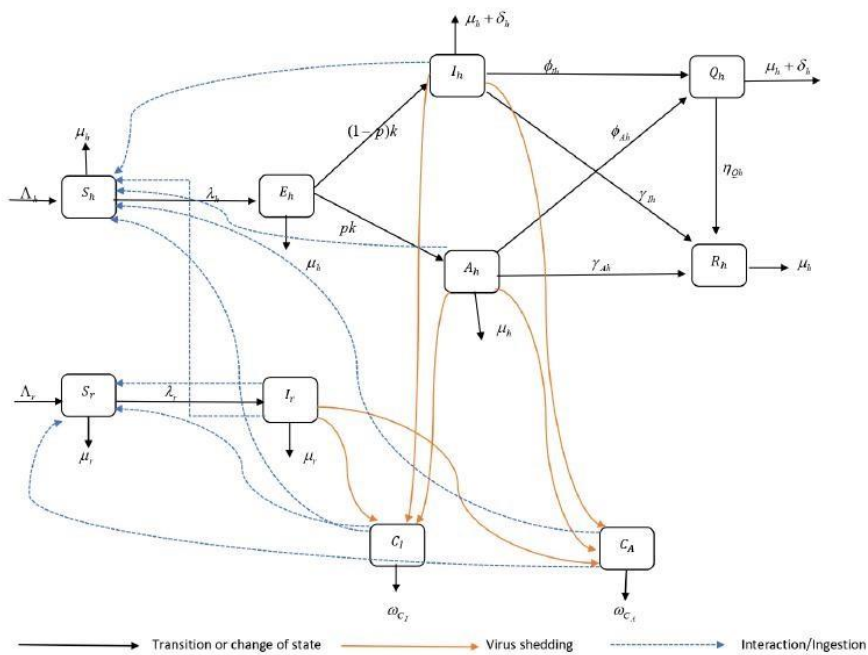


Figure 1: Model schematic diagram

3.5 Model equations

From the model schematic diagram, we obtained the following equations which describe the dynamics of each variable over time.

Human compartments:

$$\frac{dS_h}{dt} = \Lambda_h - \lambda_h S_h - \mu_h S_h, \quad (1)$$

$$\frac{dE_h}{dt} = \lambda_h S_h - (\kappa_h + \mu_h) E_h, \quad (2)$$

$$\frac{dI_h}{dt} = (1 - p)\kappa_h E_h - (\gamma_{Ih} + \mu_h + \delta_h + \phi_{Ih}) I_h, \quad (3)$$

$$\frac{dA_h}{dt} = p\kappa_h E_h - (\gamma_{Ah} + \mu_h + \phi_{Ah}) A_h, \quad (4)$$

$$\frac{dQ_h}{dt} = \phi_{Ih} I_h + \phi_{Ah} A_h - (\eta_{Qh} + \mu_h + \delta_{Qh}) Q_h, \quad (5)$$

$$\frac{dR_h}{dt} = \gamma_{Ih} I_h + \gamma_{Ah} A_h + \eta_{Qh} Q_h - \mu_h R_h, \quad (6)$$

Rodents compartments:

$$\frac{dS_r}{dt} = \Lambda_r - \lambda_r S_r - \mu_r S_r, \quad (7)$$

$$\frac{dI_r}{dt} = \lambda_r S_r - \mu_r I_r, \quad (8)$$

Environmental contamination:

$$\frac{dC_I}{dt} = \sigma_{Ih} I_h + \sigma_{Ah} A_h + \sigma_{Ir} I_r - \omega_{C_I} C_I, \quad (9)$$

$$\frac{dC_A}{dt} = \zeta_{Ih} I_h + \zeta_{Ah} A_h + \zeta_{Ir} I_r - \omega_{C_A} C_A. \quad (10)$$

The forces of infection are given by

$$\lambda_h = \beta_{hh} \frac{I_h}{N_h} + \beta_{ha} \frac{A_h}{N_h} + \beta_{rh} \frac{I_r}{N_r} + \beta_{C_{Ih}} \frac{C_I}{N_h} + \beta_{C_{Ah}} \frac{C_A}{N_h}, \quad (11)$$

$$\lambda_r = \beta_{rr} \frac{I_r}{N_r} + \beta_{C_{Ir}} \frac{C_I}{N_r} + \beta_{C_{Ar}} \frac{C_A}{N_r}, \quad (12)$$

where $N_h = S_h + E_h + I_h + A_h + Q_h + R_h$ and $N_r = S_r + I_r$.

We introduced four control measures into the model as follows:

Surveillance and case detection (u_1): enhances the isolation of symptomatic and asymptomatic infected humans, thus decreasing the infectious pool and reducing secondary human infections.

Infection-control (u_2): represents disinfection, safe waste disposal, and hospital hygiene measures that reduce items and air contamination, reducing the environmental reservoir.

Public health education (u_3): models behavioral changes such as avoiding contact with rodent excreta, proper food storage and use of protective measures in healthcare settings. This control reduces all effective transmission rates.

Rodent-targeted control (u_4): includes rodent proof, baiting and trapping activities in the community. Increase rodent removal, thereby reducing the likelihood of rodent-to-human and rodent-to-rodent transmission.

The controlled model is therefore:

Human Compartments:

$$\frac{dS_h}{dt} = \Lambda_h - \lambda_h(t)S_h - \mu_h S_h, \quad (13)$$

$$\frac{dE_h}{dt} = \lambda_h(t)S_h - (\kappa_h + \mu_h)E_h, \quad (14)$$

$$\frac{dI_h}{dt} = (1 - p)\kappa_h E_h - [\gamma_{Ih} + \mu_h + \delta_h + \phi_{Ih}(1 + \alpha_{Ih}u_1)]I_h, \quad (15)$$

$$\frac{dA_h}{dt} = p\kappa_h E_h - [\gamma_{Ah} + \mu_h + \phi_{Ah}(1 + \alpha_{Ah}u_1)]A_h, \quad (16)$$

$$\frac{dQ_h}{dt} = \phi_{Ih}(1 + \alpha_{Ih}u_1)I_h + \phi_{Ah}(1 + \alpha_{Ah}u_1)A_h - (\eta_{Qh} + \mu_h + \delta_{Qh})Q_h, \quad (17)$$

$$\frac{dR_h}{dt} = \gamma_{Ih}I_h + \gamma_{Ah}A_h + \eta_{Qh}Q_h - \mu_h R_h. \quad (18)$$

Rodents Compartments:

$$\frac{dS_r}{dt} = \Lambda_r - \lambda_r(t)S_r - (\mu_r + c_r u_4)S_r, \quad (19)$$

$$\frac{dI_r}{dt} = \lambda_r(t)S_r - (\mu_r + c_r u_4)I_r. \quad (20)$$

Environmental Contamination:

$$\frac{dC_I}{dt} = (1 - u_2)(\sigma_{Ih}I_h + \sigma_{Ah}A_h + \sigma_{Ir}I_r) - \omega_{CI}C_I, \quad (21)$$

$$\frac{dC_A}{dt} = (1 - u_2)(\zeta_{Ih}I_h + \zeta_{Ah}A_h + \zeta_{Ir}I_r) - \omega_{CA}C_A. \quad (22)$$

The time-dependent forces of infection, scaled by education u_3 , are

$$\lambda_h(t) = (1 - u_3) \left(\beta_{hh} \frac{I_h}{N_h} + \beta_{ha} \frac{A_h}{N_h} + \beta_{rh} \frac{I_r}{N_r} + \beta_{CIh} \frac{C_I}{N_h} + \beta_{CAh} \frac{C_A}{N_h} \right). \quad (23)$$

$$\lambda_r(t) = (1 - u_3) \left(\beta_{rr} \frac{I_r}{N_r} + \beta_{CIr} \frac{C_I}{N_r} + \beta_{CAr} \frac{C_A}{N_r} \right). \quad (24)$$

Here c_r is the maximum removal rate of infected rodents per unit control effort. The initial conditions are;

$$S_h(0), E_h(0), I_h(0), A_h(0), Q_h(0), R_h(0), S_r(0), I_r(0), C_I(0), C_A(0) \geq 0.$$

Together, these equations describe the dynamics of Lassa fever transmission within and between humans, rodents, and the environment, while explicitly capturing the effects of the four control strategies: u_1 (surveillance), u_2 (infection control), u_3 (public health education), and u_4 (rodent-targeted control).

3.6 Description of model equations

Each equation in the system represents the rate of change of a particular compartment within the human, rodent, or environmental populations. The model captures how individuals or compartments interact through infection, progression, recovery, and control interventions. The biological meanings of each equation are as follows:

Susceptible humans (S_h): The susceptible human population increases through recruitment at rate Λ_h and decreases due to infection at rate $\lambda_h S_h$ and natural death at rate $\mu_h S_h$.

$$\frac{dS_h}{dt} = \Lambda_h - \lambda_h S_h - \mu_h S_h$$

Exposed humans (E_h): Individuals enter the exposed class upon infection and remain there during the latent period. They progress to either symptomatic or asymptomatic infection at rate κ_h , or die naturally at rate μ_h .

$$\frac{dE_h}{dt} = \lambda_h S_h - (\kappa_h + \mu_h) E_h$$

Symptomatic infectious humans (I_h): A fraction $(1 - p)$ of exposed individuals become symptomatic. They recover at rate γ_{Ih} , die due to disease at rate δ_h , or are isolated by surveillance at rate $\phi_{Ih}(1 + \alpha_{Ih}u_1)$.

$$\frac{dI_h}{dt} = (1 - p)\kappa_h E_h - [\gamma_{Ih} + \mu_h + \delta_h + \phi_{Ih}(1 + \alpha_{Ih}u_1)]I_h$$

Asymptomatic infectious humans (A_h): A fraction p of exposed individuals develop mild or asymptomatic infections. They recover at rate γ_{Ah} , die naturally at rate μ_h , or may be isolated at rate $\phi_{Ah}(1 + \alpha_{Ah}u_1)$.

$$\frac{dA_h}{dt} = p\kappa_h E_h - [\gamma_{Ah} + \mu_h + \phi_{Ah}(1 + \alpha_{Ah}u_1)]A_h$$

Quarantined humans (Q_h): Individuals in quarantine arise from both symptomatic and asymptomatic infections through enhanced surveillance. They recover at rate η_{Qh} or die from disease or natural causes.

$$\frac{dQ_h}{dt} = \phi_{Ih}(1 + \alpha_{Ih}u_1)I_h + \phi_{Ah}(1 + \alpha_{Ah}u_1)A_h - (\eta_{Qh} + \mu_h + \delta_{Qh})Q_h$$

Recovered humans (R_h): Recovered individuals arise from recovery of symptomatic, asymptomatic, and quarantined individuals. They are assumed to have temporary or permanent immunity and die naturally at rate μ_h .

$$\frac{dR_h}{dt} = \gamma_{Ih}I_h + \gamma_{Ah}A_h + \eta_{Qh}Q_h - \mu_h R_h$$

Susceptible rodents (S_r): The susceptible rodent population grows through recruitment at rate Λ_r and declines through infection at rate $\lambda_r S_r$ and natural death at rate $\mu_r S_r$.

$$\frac{dS_r}{dt} = \Lambda_r - \lambda_r S_r - \mu_r S_r$$

Infectious rodents (I_r): Rodents become infected through contact with infectious rodents or contaminated environments. They may die naturally at the rate μ_r or be removed through rodent-targeted control u_4 with effectiveness c_r .

$$\frac{dI_r}{dt} = \lambda_r S_r - (\mu_r + c_r u_4) I_r$$

Contaminated items (C_I): This compartment represents environmental surfaces and fomites contaminated by infectious humans and rodents. The level of contamination increases through shedding rates σ_{Ih} , σ_{Ah} , and σ_{Ir} , and decays naturally at rate ω_{C_I} . Infection-control measures (u_2) reduce contamination proportionally.

$$\frac{dC_I}{dt} = (1 - u_2)(\sigma_{Ih}I_h + \sigma_{Ah}A_h + \sigma_{Ir}I_r) - \omega_{C_I} C_I$$

Contaminated aerosols (C_A): This represents airborne viral particles produced by infected humans and rodents. Contamination increases through aerosol shedding rates ζ_{Ih} , ζ_{Ah} , and ζ_{Ir} , and decreases by natural decay at rate ω_{C_A} . Infection-control measures (u_2) similarly reduce aerosol contamination.

$$\frac{dC_A}{dt} = (1 - u_2)(\zeta_{Ih}I_h + \zeta_{Ah}A_h + \zeta_{Ir}I_r) - \omega_{C_A} C_A$$

Together, these equations give the dynamics of Lassa fever virus over time, in the presence of control strategies. To check the robustness and adaptability of our model in performing the intended task, we test the model through qualitative and quantitative analysis, the results can be found in the next section.

4 Results and Discussions

We performed qualitative and quantitative analysis on the model by stating and proving some results in relation to our model equations, and performing numerical simulations in order to visualize the impact of the controls we introduced in the model.

4.1 Qualitative analysis

4.1.1 Positivity and boundedness of solutions

Theorem 1 (Positivity and boundedness). *Let $u_i \in [0, 1]$ be measurable bounded controls and let the parameters $\Lambda_h, \Lambda_r, \mu_h, \mu_r, \kappa_h, p, \gamma_{Ih}, \gamma_{Ah}, \gamma_{Ir}, \delta_h, \delta_r, \phi_{Ih}, \phi_{Ah}, \dots$, be nonnegative. For any initial condition*

$$\mathbf{X}(0) = (S_h(0), E_h(0), I_h(0), A_h(0), Q_h(0), R_h(0), S_r(0), I_r(0), C_I(0), C_A(0))$$

with non-negative components, the unique solution $\mathbf{X}(t)$ of the model exists for all $t \geq 0$ and satisfies:

1. Positivity: $S_h(t), E_h(t), I_h(t), A_h(t), Q_h(t), R_h(t), S_r(t), I_r(t), C_I(t), C_A(t) \geq 0$ for all $t \geq 0$.
2. Uniform boundedness: the total human and rodent populations satisfy

$$\limsup_{t \rightarrow \infty} N_h(t) \leq \frac{\Lambda_h}{\mu_h}, \quad \limsup_{t \rightarrow \infty} N_r(t) \leq \frac{\Lambda_r}{\mu_r},$$

where $N_h(t) = S_h + E_h + I_h + A_h + Q_h + R_h$ and $N_r(t) = S_r + I_r$. Hence all state variables are uniformly bounded for $t \geq 0$ and trajectories remain in the feasible region

$$\Omega = \left\{ (x_i) \in \mathbb{R}_+^{10} : 0 \leq N_h \leq \frac{\Lambda_h}{\mu_h}, 0 \leq N_r \leq \frac{\Lambda_r}{\mu_r}, C_I, C_A \geq 0 \right\}.$$

Proof. (Positivity) Let the initial conditions be nonnegative:

$$S_h(0), E_h(0), I_h(0), A_h(0), Q_h(0), R_h(0), S_r(0), I_r(0), C_I(0), C_A(0) \geq 0.$$

The right-hand sides of the model equations are continuous and locally Lipschitz on \mathbb{R}_+^{10} . We want to show that each state variable cannot become negative if it starts non-negative. Each compartment can be expressed in the form:

$$\frac{dx_i}{dt} = \text{inflow terms} - \text{outflow terms}.$$

At any time when $x_i = 0$, the outflow terms vanish while inflow terms are nonnegative. Therefore, $\frac{dx_i}{dt} \geq 0$, which ensures $x_i(t)$ remains nonnegative for all $t > 0$.

(Boundedness) Define total human and rodents population $N_h = S_h + E_h + I_h + A_h + Q_h + R_h$, and $N_r = S_r + I_r$. Adding the corresponding human and rodents equations gives

$$\frac{dN_h}{dt} = \Lambda_h - \mu_h N_h - \delta_h (I_h + Q_h), \quad \frac{dN_r}{dt} = \Lambda_r - \mu_r N_r.$$

since recovery terms transfer between human compartments and cancel in the sum. Because $\delta_h(I_h + Q_h) \geq 0$, we obtain the differential inequalities

$$\frac{dN_h}{dt} \leq \Lambda_h - \mu_h N_h, \quad \frac{dN_r}{dt} \leq \Lambda_r - \mu_r.$$

Consider the linear scalar comparison equation $y' = \Lambda_h - \mu_h y$ with solution

$$y(t) = y(0)e^{-\mu_h t} + \frac{\Lambda_h}{\mu_h}(1 - e^{-\mu_h t}).$$

By the comparison principle, $N_h(t) \leq y(t)$, hence we obtain:

$$N_h(t) \leq \frac{\Lambda_h}{\mu_h} + (N_h(0) - \frac{\Lambda_h}{\mu_h})e^{-\mu_h t}, \quad N_r(t) \leq \frac{\Lambda_r}{\mu_r} + (N_r(0) - \frac{\Lambda_r}{\mu_r})e^{-\mu_r t}.$$

$$\limsup_{t \rightarrow \infty} N_h(t) \leq \frac{\Lambda_h}{\mu_h}, \quad \limsup_{t \rightarrow \infty} N_r(t) \leq \frac{\Lambda_r}{\mu_r}.$$

Hence, N_h and N_r are bounded above by Λ_h/μ_h and Λ_r/μ_r , respectively. Environmental compartments C_I and C_A are also bounded, since:

$$\frac{dC_I}{dt} = \sigma_{Ih}I_h + \sigma_{Ah}A_h + \sigma_{Ir}I_r - \omega_{C_I}C_I, \quad \frac{dC_A}{dt} = \zeta_{Ih}I_h + \zeta_{Ah}A_h + \zeta_{Ir}I_r - \omega_{C_A}C_A,$$

with bounded forcing terms I_h , A_h , and I_r .

Therefore, all solutions of the model are positive and remain in the positively invariant region:

$$\Omega = \left\{ (x_i) \in \mathbb{R}_+^{11} : 0 \leq N_h \leq \frac{\Lambda_h}{\mu_h}, 0 \leq N_r \leq \frac{\Lambda_r}{\mu_r}, C_I, C_A \geq 0 \right\}.$$

□

4.1.2 Disease-Free Equilibrium (DFE)

The DFE, denoted by E_0 , is obtained by setting all infected compartments and the model equations to zero:

$$E_0 = \left(S_h^0 = \frac{\Lambda_h}{\mu_h}, E_h^0 = I_h^0 = A_h^0 = Q_h^0 = R_h^0 = 0, S_r^0 = \frac{\Lambda_r}{\mu_r}, E_r^0 = I_r^0 = C_I^0 = C_A^0 = 0 \right).$$

4.1.3 Basic/Controlled reproduction number

Because controls u_i are treated as constant parameters, we compute the basic/controlled (or intervention-adjusted) reproduction number \mathcal{R}_c by evaluating the next-generation matrix at the disease-free equilibrium with the chosen control levels. To compute the reproduction number, we use the next generation matrix method, given as

$$\mathcal{R}_c = \rho(FV^{-1}),$$

which we write here as $\mathcal{R}_c = \rho(K)$, where $\rho(K)$ denotes the spectral radius of $K = FV^{-1}$.
 Let the infected-state vector be

$$\mathbf{y} = (E_h, I_h, A_h, I_r)^T.$$

The subsystem of infected equations extracted from the full model can be written as

$$\frac{d\mathbf{y}}{dt} = \mathcal{F}(\mathbf{y}) - \mathcal{V}(\mathbf{y}),$$

where \mathcal{F} represents the appearance of new infections and \mathcal{V} represents all other transitions among infected compartments.

The Vector of new infection terms $\mathcal{F}(\mathbf{y})$ and that of transition terms $\mathcal{V}(\mathbf{y})$ are given as:

$$\mathcal{F}(\mathbf{y}) = \begin{pmatrix} (1-u_3)\left(\beta_{hh}\frac{I_h}{N_h} + \beta_{ha}\frac{A_h}{N_h} + \beta_{rh}\frac{I_r}{N_r} + \beta_{C_{Ih}}\frac{C_I}{N_h} + \beta_{C_{Ah}}\frac{C_A}{N_h}\right)S_h \\ 0 \\ 0 \\ (1-u_3)\left(\beta_{rr}\frac{I_r}{N_r}S_r + \beta_{C_{Ih}}\frac{C_I}{N_h} + \beta_{C_{Ah}}\frac{C_A}{N_h}\right) \end{pmatrix}, \quad \mathcal{V}(\mathbf{y}) = \begin{pmatrix} (\kappa_h + \mu_h)E_h \\ d_{I_h}I_h - (1-p)\kappa_hE_h \\ d_{A_h}A_h - p\kappa_hE_h \\ d_{I_r}I_r \end{pmatrix},$$

where

$$\begin{aligned} d_{I_h} &= \gamma_{I_h} + \mu_h + \delta_h + \varphi_{I_h}(1 + \alpha_{I_h}u_1), \\ d_{A_h} &= \gamma_{A_h} + \mu_h + \varphi_{A_h}(1 + \alpha_{A_h}u_1), \\ d_{I_r} &= \mu_r + c_r u_4. \end{aligned}$$

At the disease-free equilibrium E_0 , where $S_h = N_h$ and $S_r = N_r$,

$$F = \begin{pmatrix} 0 & (1-u_3)\beta_{hh} & (1-u_3)\beta_{ha} & (1-u_3)\beta_{rh} \\ 0 & 0 & 0 & 0 \\ 0 & 0 & 0 & 0 \\ 0 & 0 & 0 & (1-u_3)\beta_{rr} \end{pmatrix}, \quad V = \begin{pmatrix} \kappa_h + \mu_h & 0 & 0 & 0 \\ -(1-p)\kappa_h & d_{I_h} & 0 & 0 \\ -p\kappa_h & 0 & d_{A_h} & 0 \\ 0 & 0 & 0 & d_{I_r} \end{pmatrix}.$$

The inverse of V is

$$V^{-1} = \begin{pmatrix} \frac{1}{\kappa_h + \mu_h} & 0 & 0 & 0 \\ \frac{\kappa_h(1-p)}{(\kappa_h + \mu_h)d_{I_h}} & \frac{1}{d_{I_h}} & 0 & 0 \\ \frac{\kappa_h p}{(\kappa_h + \mu_h)d_{A_h}} & 0 & \frac{1}{d_{A_h}} & 0 \\ 0 & 0 & 0 & \frac{1}{d_{I_r}} \end{pmatrix},$$

and the next-generation matrix $K = FV^{-1}$ is

$$K = \begin{pmatrix} K_{11} & \frac{(1-u_3)\beta_{hh}}{d_{Ih}} & \frac{(1-u_3)\beta_{ha}}{d_{Ah}} & \frac{(1-u_3)\beta_{rh}}{d_{Ir}} \\ 0 & 0 & 0 & 0 \\ 0 & 0 & 0 & 0 \\ 0 & 0 & 0 & \frac{(1-u_3)\beta_{rr}}{d_{Ir}} \end{pmatrix},$$

where

$$K_{11} = (1-u_3) \frac{\kappa_h}{\kappa_h + \mu_h} \left((1-p) \frac{\beta_{hh}}{d_{Ih}} + p \frac{\beta_{ha}}{d_{Ah}} \right).$$

Hence,

$$R_c = \rho(K) = \max\{K_{11}, K_{44}\}, \quad \text{with} \quad K_{44} = \frac{(1-u_3)\beta_{rr}}{d_{Ir}}.$$

A convenient decomposition highlights the major contributions:

$$\mathcal{R}_c \approx (1-u_3) \left[\frac{\beta_{hh}(1-p)\kappa_h}{(\kappa_h + \mu_h)d_{Ih}} + \frac{\beta_{ha}p\kappa_h}{(\kappa_h + \mu_h)d_{Ah}} \right] + (1-u_3) \frac{\beta_{rr}}{d_{Ir}},$$

where the first two terms represent symptomatic and asymptomatic human transmissions and the last term corresponds to the rodent contribution including the rodent-targeted control u_4 which increases d_{Ir} and hence reduces \mathcal{R}_0 .

4.1.4 Local stability of the Disease-Free Equilibrium

We check for local stability using the Routh-Hurwitz condition. We start by formulating the Jacobian matrix for the infected subsystem, and the linearization is restricted to infected variables as

$$J_{\text{infected}} = F - V = \begin{pmatrix} -(\kappa + \mu) & (1-u_3)\beta_{hh} & (1-u_3)\beta_{ha} & (1-u_3)\beta_{rh} \\ (1-p)\kappa & -d_{Ih} & 0 & 0 \\ p\kappa & 0 & -d_{Ah} & 0 \\ 0 & 0 & 0 & (1-u_3)\beta_{rr} - d_{Ir} \end{pmatrix}.$$

Because this is block-triangular, the characteristic polynomial factorises as

$$\det(\lambda I - J_{\text{infected}}) = P_3(\lambda) (\lambda - ((1-u_3)\beta_{rr} - d_{Ir})),$$

where $P_3(\lambda)$ is the cubic characteristic polynomial of the human square block

$$M_3 = \begin{pmatrix} -(\kappa + \mu) & (1-u_3)\beta_{hh} & (1-u_3)\beta_{ha} \\ (1-p)\kappa & -d_{Ih} & 0 \\ p\kappa & 0 & -d_{Ah} \end{pmatrix}.$$

The cubic characteristic polynomial is given as

$$P_3(\lambda) = \det(\lambda I - M_3) = \lambda^3 + a_1\lambda^2 + a_2\lambda + a_3.$$

The coefficients (a_1, a_2, a_3) are obtained by direct expansion as:

$$\begin{aligned} a_1 &= d_{A_h} + d_{I_h} + \kappa + \mu. \\ a_2 &= d_{A_h}d_{I_h} + (\kappa + \mu)(d_{I_h} + d_{A_h}) - (1 - u_3)\kappa\left((1 - p)\beta_{hh} + p\beta_{ha}\right). \\ a_3 &= (\kappa + \mu)d_{I_h}d_{A_h} - (1 - u_3)\kappa\left((1 - p)d_{A_h}\beta_{hh} + p d_{I_h}\beta_{ha}\right). \end{aligned}$$

The Routh–Hurwitz conditions for the cubic polynomial is

$$\lambda^3 + a_1\lambda^2 + a_2\lambda + a_3,$$

where all roots have negative real parts (equivalently the 3×3 human block is Hurwitz) if and only if the following Routh–Hurwitz conditions hold:

$$a_1 > 0, \quad a_2 > 0, \quad a_3 > 0, \quad a_1a_2 > a_3.$$

From our model, $a_1 > 0$ automatically holds because $d_{A_h}, d_{I_h}, \kappa, \mu$ are positive rates. The non-trivial algebraic inequalities are $a_2 > 0$, $a_3 > 0$, and $a_1a_2 > a_3$. We Observe that a_3 can be rewritten as

$$a_3 = (\kappa + \mu)d_{I_h}d_{A_h} - (\kappa + \mu)d_{I_h}d_{A_h} \cdot \underbrace{\left[(1 - u_3)\frac{\kappa}{\kappa + \mu} \left((1 - p)\frac{\beta_{hh}}{d_{I_h}} + p\frac{\beta_{ha}}{d_{A_h}} \right) \right]}_{=K_{11}}.$$

Dividing both sides by $(\kappa + \mu)d_{I_h}d_{A_h} > 0$ gives the exact equivalence

$$a_3 > 0 \iff K_{11} < 1.$$

Thus the Routh–Hurwitz scalar condition $a_3 > 0$ is precisely the same threshold condition obtained from the next-generation human contribution K_{11} .

Similarly, the scalar factor $\lambda - ((1 - u_3)\beta_{rr} - d_{I_r})$ (rodents specific) gives eigenvalue

$$\lambda_4 = (1 - u_3)\beta_{rr} - d_{I_r}.$$

This eigenvalue has negative real part iff $(1 - u_3)\beta_{rr} - d_{I_r} < 0 \iff \frac{(1 - u_3)\beta_{rr}}{d_{I_r}} < 1$, i.e. $K_{44} < 1$.

Collecting the cubic Routh–Hurwitz conditions and the rodent scalar condition, the disease-free equilibrium is locally asymptotically stable if and only if

$$\begin{cases} a_1 > 0, a_2 > 0, \\ a_3 > 0 \quad (\iff K_{11} < 1), \\ a_1 a_2 > a_3, \\ K_{44} < 1. \end{cases}$$

Because $a_1 > 0$ automatically, the key epidemiological threshold conditions reduce to $K_{11} < 1$ and $K_{44} < 1$, i.e. $\max\{K_{11}, K_{44}\} < 1$.

Hence, it is locally asymptotically stable since $R_e = \rho(K) < 1$.

4.1.5 Global stability of the Disease-Free Equilibrium (DFE)

The global behavior of the system when $\mathcal{R}_0 < 1$ can be established using the decomposition approach of Castillo-Chavez and Song (2004) and the next-generation framework of van den Driessche and Watmough (2002).

Let the system be partitioned as

$$\dot{\mathbf{x}} = f(\mathbf{x}, \mathbf{y}), \quad \dot{\mathbf{y}} = g(\mathbf{x}, \mathbf{y}),$$

where \mathbf{x} represents the uninfected compartments (S_h, S_r, R_h, Q_h) and $\mathbf{y} = (E_h, I_h, A_h, I_r)^\top$ the infected subsystem. The disease-free equilibrium (DFE) is

$$E_0 = (S_h^0, 0, 0, 0, 0, 0, S_r^0, 0, 0, 0), \quad S_h^0 = \frac{\Lambda_h}{\mu_h}, \quad S_r^0 = \frac{\Lambda_r}{\mu_r}.$$

In the absence of infection ($\mathbf{y} = \mathbf{0}$), the human and rodent populations follow linear differential equations with globally attracting equilibria at S_h^0 and S_r^0 . Hence the uninfected subsystem is globally asymptotically stable.

The infected equations can be written as

$$\dot{\mathbf{y}} = \mathcal{F}(\mathbf{x}, \mathbf{y}) - \mathcal{V}(\mathbf{x}, \mathbf{y}),$$

where \mathcal{F} denotes new infections and \mathcal{V} all transitions and removals. At the DFE, let $F = D_{\mathbf{y}}\mathcal{F}(E_0)$ and $V = D_{\mathbf{y}}\mathcal{V}(E_0)$, so that $\mathcal{R}_0 = \rho(FV^{-1})$.

Because susceptibles satisfy $S_h(t) \leq S_h^0$ and $S_r(t) \leq S_r^0$ for all sufficiently large t , it follows that $F(\mathbf{x}(t)) \leq F$ and $V(\mathbf{x}(t)) \geq V$ (componentwise). Hence the infected subsystem satisfies

$$\dot{\mathbf{y}}(t) \leq (F - V)\mathbf{y}(t). \tag{1}$$

The matrix V is an M -matrix (positive diagonal, non-positive off-diagonals as in the case of local stability).

When $\mathcal{R}_0 = \rho(FV^{-1}) < 1$, the matrix $A = F - V$ is Hurwitz; all eigenvalues have negative real parts, and the linear comparison system $\dot{\mathbf{z}} = A\mathbf{z}$ is exponentially stable.

By the comparison principle for cooperative systems,

$$\mathbf{0} \leq \mathbf{y}(t) \leq e^{A(t-T_1)}\mathbf{y}(T_1)$$

for all $t \geq T_1$, where T_1 is large enough that $S_h(t) \leq S_h^0$, $S_r(t) \leq S_r^0$. Exponential stability of A then gives $\mathbf{y}(t) \rightarrow \mathbf{0}$ as $t \rightarrow \infty$.

Since the infected components vanish asymptotically and the uninfected subsystem converges to (S_h^u, S_r^u) , the full solution tends to

$$\mathbf{X}(t) = (\mathbf{x}(t), \mathbf{y}(t)) \rightarrow (\mathbf{x}^*, \mathbf{0}) = E_0.$$

Thus, the DFE is globally asymptotically stable whenever $\mathcal{R}_0 < 1$.

The result implies that, provided the combined control efforts (surveillance u_1 , infection-control u_2 , public health education u_3 , and rodent-targeted control u_4) are strong enough to keep \mathcal{R}_0 below unity, all infections in humans and rodents eventually die out and the disease cannot invade the population.

4.1.6 Existence of Endemic Equilibrium (EE)

When $\mathcal{R}_c > 1$, the model admits at least one positive endemic equilibrium

$$E^* = (S_h^*, E_h^*, I_h^*, A_h^*, Q_h^*, R_h^*, S_r^*, E_r^*, I_r^*, C_I^*, C_A^*),$$

which satisfies the steady-state equations obtained by setting $\dot{x} = 0$.

4.2 Quantitative analysis

4.2.1 Parameter estimation and baseline values

Parameter values used for numerical simulations were obtained from published literature on Lassa fever modeling and related zoonotic diseases, as well as from epidemiological data reported by the Nigeria Centre for Disease Control (NCDC) and the World Health Organization (WHO). Biologically feasible assumptions were also made to maintain model realism and dimensional consistency. Rates such as recovery, natural death, and progression were derived from typical infectious period durations. Transmission coefficients were chosen to ensure that the basic reproduction number (R_0) under the baseline scenario exceeds unity in the absence of controls, reflecting an endemic state consistent with observed outbreaks in Nigeria. Environmental parameters such as shedding and decay rates were adapted from studies that modeled pathogen persistence in contaminated environments. The baseline parameter values used in this study are summarized in Table 3, 4, and the initial values as well as the controls are in Table 5.

Table 3: Epidemiological parameters used for the Lassa fever model (Nigeria case study).

Symbol	Description	Value	Unit	Source/Remark
N_h	Initial human population	2.0×10^8	persons	Estimated Nigeria population (James et al., 2023)
N_r	Initial rodent population	1.0×10^7	rodents	Approximate reservoir estimate
Λ_h	Human recruitment rate	$\mu_h N_h$	persons/day	Constant population assumption
Λ_r	Rodent recruitment rate	$\mu_r N_r$	rodents/day	Constant population assumption
μ_h	Natural death rate (humans)	$1/(54 \times 365)$	day ⁻¹	Life expectancy \approx 54 years (James et al., 2023)
μ_r	Natural death rate (rodents)	0.0038	day ⁻¹	James et al., 2023)
κ_h	Incubation rate (exposed \rightarrow infectious)	1/10	day ⁻¹	10-day incubation (WHO, 2024).
p	Fraction asymptomatic	0.8	–	Epidemiological estimate
γ_{I_h}	Recovery rate (symptomatic humans)	1/12	day ⁻¹	Infectious period \approx 12 days (WHO, 2023).
γ_{A_h}	Recovery rate (asymptomatic humans)	1/7	day ⁻¹	Faster recovery for mild infection (assumed)
δ_h	Disease-induced mortality (humans)	0.002	day ⁻¹	Case fatality \approx 0.2% (Dohan et al., 2024).
ϕ_{I_h}	Detection/isolation rate (symptomatic)	0.05	day ⁻¹	Moderate surveillance level (assumed)
ϕ_{A_h}	Detection/isolation rate (asymptomatic)	0.01	day ⁻¹	Low detection for mild cases (assumed)
η_{Q_h}	Recovery rate of quarantined humans	1/7	day ⁻¹	Quarantine period \approx 7 days (assumed)

Table 4: Environmental and transmission parameters for the Lassa fever model.

Symbol	Description	Value	Unit	Source/Remark
σ_{I_h}	Shedding rate of I_h to items	1.0	–	Environmental contamination rate (assumed)
σ_{A_h}	Shedding rate of A_h to items	0.5	–	Reduced relative to I_h (assumed)
σ_{I_r}	Shedding rate of I_r to items	0.8	–	Rodent contamination (assumed)
ζ_{I_h}	Shedding rate of I_h to aerosols	0.8	–	Aerosol contamination (assumed)
ζ_{A_h}	Shedding rate of A_h to aerosols	0.4	–	Mildly infectious aerosols (assumed)
ζ_{I_r}	Shedding rate of I_r to aerosols	0.6	–	Rodent contribution (assumed)
ω_{C_I}	Decay rate of contaminated items	1/48	day ⁻¹	Assumed
ω_{C_A}	Decay rate of contaminated aerosols	1/0.5	day ⁻¹	Half-life \approx 12 hours (assumed)
β_{hh}	Transmission (human-to-human, symptomatic)	0.6	day ⁻¹	High infectivity (assumed)
β_{ha}	Transmission (human-to-human, asymptomatic)	0.3	day ⁻¹	Mild infectivity (assumed)
β_{rh}	Transmission (rodent-to-human)	0.05	day ⁻¹	Food/household contamination (assumed)
β_{rr}	Transmission (rodent-to-rodent)	0.4	day ⁻¹	High intra-species contact (assumed)
β_{C_Ih}	Transmission (contaminated items \rightarrow humans)	0.03	day ⁻¹	Indirect exposure (assumed)
β_{C_Ah}	Transmission (contaminated aerosols \rightarrow humans)	0.02	day ⁻¹	Inhalation exposure (assumed)
β_{C_Ir}	Transmission (items \rightarrow rodents)	0.025	day ⁻¹	Environmental contact (assumed)
β_{C_Ar}	Transmission (aerosols \rightarrow rodents)	0.015	day ⁻¹	Low probability (assumed)

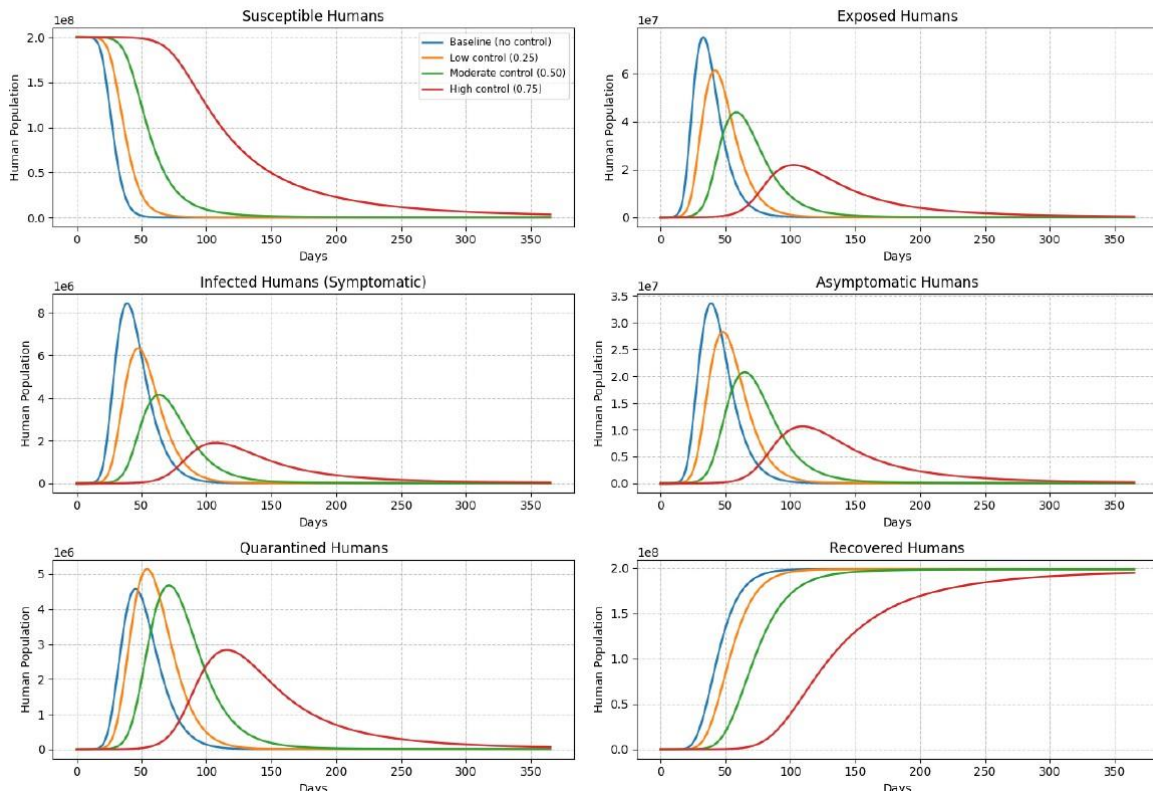
Table 5: Control parameters and initial conditions for the simulation.

Symbol	Description	Value	Unit	Remark
c_r	Additional rodent mortality under control	0.05	day ⁻¹	Reflects rodenticide/trapping
α_{I_h}	Effect of control on symptomatic detection	2.0	–	Amplifies ϕ_{I_h} by u_1
α_{A_h}	Effect of control on asymptomatic detection	1.0	–	Amplifies ϕ_{A_h} by u_1
$S_h(0)$	Initial susceptible humans	$2.0 \times 10^8 - 1500$	persons	Majority of population
$E_h(0)$	Initial exposed humans	800	persons	Early incubation
$I_h(0)$	Initial symptomatic humans	500	persons	Infectious at baseline
$A_h(0)$	Initial asymptomatic humans	200	persons	Mild infection
$Q_h(0)$	Initial quarantined humans	100	persons	Early isolation cases
$R_h(0)$	Initial recovered humans	0	persons	None initially immune
$S_r(0)$	Initial susceptible rodents	$1.0 \times 10^7 - 2000$	rodents	Majority uninfected
$I_r(0)$	Initial infected rodents	2000	rodents	Persistent reservoir
$C_I(0)$	Initial contaminated items	300	–	Low background contamination
$C_A(0)$	Initial contaminated aerosols	50	–	Minimal airborne presence

4.2.2 Numerical simulations

Using our baseline parameter values and initial conditions, we performed numerical simulations on the model to see the impact of the control strategies on the model dynamics over time. The simulation plot is given in Figure 2.

Lassa Fever Model (Nigeria) — 10 Compartment Dynamics under Control Scenarios



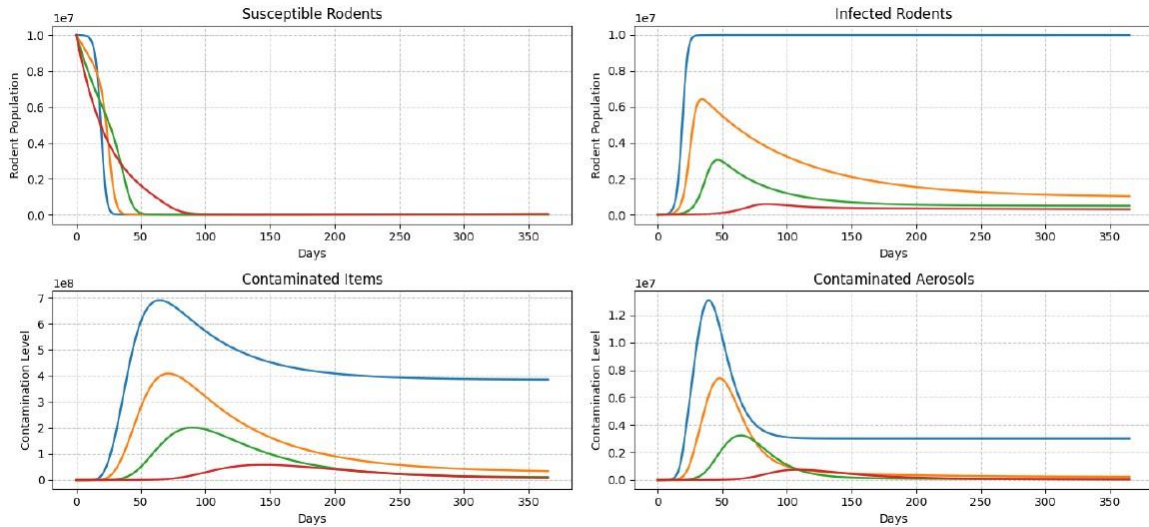


Figure 2: Simulated dynamics of the ten compartments of the Lassa fever model under baseline, low, moderate, and high control scenarios for a period of one year. The curves represent human, rodent, and environmental populations respectively.

4.3 Discussion of results

The model was simulated for a period of one year (365 days) under four control scenarios: baseline (no control), low control ($u_i = 0.25$), moderate control ($u_i = 0.50$), and high control ($u_i = 0.75$).

Human dynamics: Under the baseline scenario, the susceptible human population S_h declines rapidly at the onset of the epidemic due to high force of infection from symptomatic, asymptomatic, and rodent sources. The exposed (E_h) and infectious (I_h and A_h) populations rise sharply, indicating fast transmission. However, as control measures are implemented, infection incidence decreases markedly. With moderate and high controls, S_h remains nearly constant, while both E_h and I_h exhibit lower and shorter peaks, signifying effective containment. The quarantined population Q_h initially peaks higher under low control than at baseline. This occurs because partial control enhances case detection and isolation ($u_1 > 0$) while infection prevalence remains relatively high. Thus, more individuals are transferred to quarantine temporarily. At higher control levels, both infection and detection stabilize, leading to lower quarantine peaks. This non-monotonic behaviour is biologically realistic, as improving detection while transmission is still active transiently increases quarantine numbers before eventual epidemic decline. The recovered class R_h increases with time as individuals leave the infectious and quarantined compartments. Under high control, recovery dominates over new infections, leading to eventual disease fade-out.

Rodent dynamics: For rodents, the susceptible class S_r declines slowly due to persistent contact with contaminated environments and infected rodents, while the infectious rodent population I_r rises and stabilizes. Introduction of control u_4 (rodent removal) significantly reduces I_r , especially under moderate and high control scenarios, confirming the importance of rodent population management in Lassa fever control.

Environmental compartments: Both C_I (contaminated items) and C_A (contaminated aerosols) follow the trends of the infectious classes. They peak during the early epidemic phase and decay gradually as shedding sources diminish and sanitation control (u_2) increases. Because aerosols decay faster than items, C_A exhibits a lower and earlier peak.

Reproduction numbers and control impact: Using the model parameters, the basic reproduction number R_0 for Nigeria was estimated as approximately $R_0 \approx 2.47$, implying that one infectious case generates about two to three secondary cases in a fully susceptible population. Under increasing control intensities, the controlled reproduction number R_c decreases progressively. For instance:

Baseline: $R_c \approx 2.47$, Low control: $R_c \approx 1.47$, Moderate control: $R_c \approx 0.88$, High control: $R_c \approx 0.52$.

These correspond to reductions of approximately 40%, 64%, and 79% in R_c relative to baseline. The declines below unity in the presence of moderate to high controls, indicate that infection eventually dies out in the long run. This is consistent with the results obtained from the qualitative analysis which showed that the model is locally and globally asymptotically stable in the presence of control strategies.

5. Conclusion

The simulations reveal that simultaneous implementation of human-related interventions (early diagnosis, quarantine, and treatment), environmental sanitation, contact reduction, and rodent control are crucial for reducing Lassa fever transmission. Partial control may increase quarantine load due to enhanced detection, but sustained moderate or high control levels ensure that both human and rodent infections decline steadily, and environmental contamination is minimized. Therefore, integrated control efforts are essential for achieving effective and sustainable Lassa fever eradication in Nigeria.

References

- Adegboye, A. R. A., Iboi, E. A., and Okuonghae, D. (2022). Modeling the impact of environmental contamination and multiple interventions on Lassa fever transmission dynamics. *Mathematical Biosciences and Engineering*, 19(5), 5101–5123.
- Anderson, R. M., & May, R. M. (1992). *Infectious Diseases of Humans: Dynamics and Control*. Oxford University Press.
- Castillo-Chavez, C., and Song, B. (2004). Dynamical models of tuberculosis and their applications. *Mathematical Biosciences and Engineering*, 1(2), 361–404.
- Diekmann, O., Heesterbeek, H., & Britton, T. (2013). *Mathematical Tools for Understanding Infectious Disease Dynamics*. Princeton University Press.
- Dohan, S., Emmanuel, M. T., and Ahmed, K. (2024). Clinical outcomes and case fatality rates of Lassa fever in Nigeria: A multi-year review. *International Journal of Infectious Diseases*, 142, 105123.
- Fichet-Calvet, E., & Rogers, D. J. (2009). Risk maps of Lassa fever in West Africa. *PLoS Neglected Tropical Diseases*, 3(3), e388.
- Fraser, C., Riley, S., Anderson, R. M., & Ferguson, N. M. (2004). Factors that make an infectious disease outbreak controllable. *Proceedings of the National Academy of Sciences*, 101(16), 6146–6151.
- Gibb, R., Moses, L. M., Redding, D. W., and Jones, K. E. (2017). Understanding the cryptic nature of Lassa fever in West Africa. *Nature Reviews Microbiology*, 15(10), 613–624.
- Iboi, E. A., Okuonghae, D., and Gumel, A. B. (2020). Mathematical assessment of the role of asymptomatic infections and environmental contamination on the transmission dynamics of Lassa fever. *Infectious Disease Modelling*, 5, 398–415.
- Lenhart, S., & Workman, J. T. (2007). *Optimal Control Applied to Biological Models*. Chapman & Hall/CRC.
- McCormick, J. B., King, I. J., Webb, P. A., Scribner, C. L., Craven, R. B., Johnson, K. M., Elliott, L. H., & Belmont-Williams, R. (1987). Lassa fever: Effective therapy with ribavirin. *New England Journal of Medicine*, 314(1), 20–26.

- McKendrick, J. Q., Tennant, W. S. D., and Tildesley, M. J. (2023). Modelling seasonality of Lassa fever incidences and vector dynamics in Nigeria. *PLOS Neglected Tropical Diseases*, 17(11): e0011543. doi:10.1371/journal.pntd.0011543.
- Nigeria Centre for Disease Control (NCDC). (2024). Weekly Epidemiological Report on Lassa Fever Outbreak in Nigeria. Abuja: NCDC.
- Ojo, M.M., Gbadamosi, B., Benson, T.O. , Adebimpe, O. & Georgina, A. L. (2021). Modeling the dynamics of Lassa fever in Nigeria. *J. Egypt Math Soc* 29, 16. <https://doi.org/10.1186/s42787-021-00124-9>.
- Richmond, J. K., & Baglole, D. J. (2003). Lassa fever: Epidemiology, clinical features, and social consequences. *BMJ*, 327(7426), 1271–1275.
- van den Driessche, P., and Watmough, J. (2002). Reproduction numbers and subthreshold endemic equilibria for compartmental models of disease transmission. *Mathematical Biosciences*, 180(1–2), 29–48.
- World Health Organization (WHO). (2017). Lassa fever: *Fact sheet*. WHO Press.
- World Health Organization (WHO). (2023). Lassa Fever *Fact Sheet*. Geneva: WHO. Available at: <https://www.who.int/newsroom/fact-sheets/detail/lassa-fever>
- World Health Organization (WHO). (2024). Lassa Fever Situation Report – 2024 Update. Geneva: *WHO Health Emergencies Programme*.